An Efficient Algorithm for Fault Location on Mixed Line-Cable Transmission Corridors

Marjan Popov, Gert Rietveld, Zoran Radojevic and Vladimir Terzija

ABSTRACT

This paper presents a fault location algorithm that can be used to accurately locate the fault at any place along mixed line-cable transmission corridors. The algorithm is an impedance based line/cable parameter dependent algorithm. The fault location algorithm is derived using distributed line model, modal transformation theory and Discrete Fourier Transform. The algorithm can be used as an on-line, or off-line application in practice. The proposed solution has the ability to locate the fault whether it is on the overhead line or on the underground power cable. The paper presents the results of the initial algorithm testing through the use of ATP simulations. Some results are validated by experimental measurements.

Key words: fault location, mixed line-cable transmission corridors, numerical algorithms, measurements, errors

I. INTRODUCTION

Overhead transmission lines, combined with underground cables, become an important issue in transmission and distribution systems. In dense populated countries and big cities, a solution for future extension of the network is seen in the application of heavily loaded cables. These cables will be connected to the existing overhead lines. The probability of occurrence of faults is however higher to happen on overhead lines than on cables. The faults may be caused by lightning strokes, falling trees, electrical breakdown of polluted insulators. Ice and snow loading may also cause insulator strings to fail mechanically. Underground cable faults may be series faults in which the cable is physically cut, or faults caused by breakdown of insulation because of overvoltage. Determination of the fault location in electric power lines is important for a secure operation of power systems. Some advantages could be: quicker repair, improved system availability, reduced operating costs and shorter time for searching the fault during severe weather conditions. So far there has been a lot of research done on fault location. Two important methods are generally accepted for fault location; that is a method based on the measurement of post-fault line impedance called phasor-based algorithms that make use only the fundamental components of the measured signals [1,2] and fault location methods based on travelling waves [3], which occur when the fault is initiated. Some other fault location techniques are summarized in [4-6].

In this paper, an impedance-based parameter dependent algorithm will be presented. The results will be demonstrated for single-phase, double-phase and three-phase fault current for different locations along a mixed line/cable transmission corridor.

II. IMPEDANCE BASED FAULT LOCATION ALGORITHM

Based on the Telegraphers' equations, voltages and currents at any place along a line can be evaluated by:

$$\begin{aligned} \frac{\partial v}{\partial x} + L\frac{\partial i}{\partial t} &= -Ri \\ C\frac{\partial i}{\partial x} + \frac{\partial v}{\partial t} &= -Gi \end{aligned} \tag{1}$$

where R, L, C and G are resistance, inductance, capacitance and conductance per unit length of the line. The solution of these equation is:

$$\begin{bmatrix} V_x \\ I_x \end{bmatrix} = \begin{bmatrix} \cosh(\gamma x) & Z_C \sinh(\gamma x) \\ \sinh(\gamma x)/Z_C & \cosh(\gamma x) \end{bmatrix} \begin{bmatrix} V_R \\ I_R \end{bmatrix} \tag{2}$$

in which, V_x, I_x are the voltage and current at distance x from the sending end of the line and V_R, I_R are the voltages and currents at the sending end. In (2),

$$Z_C = \sqrt{(R + j\omega L)/(G + j\omega C)} \text{ and } \gamma = \sqrt{(R + j\omega L)(G + j\omega C)}\,.$$

Equation (2) can also be exspressed in terms of the receiving end voltages and currents V_S, I_S, as follows:

$$\begin{bmatrix} V_x \\ I_x \end{bmatrix} = \begin{bmatrix} \cosh(\gamma(l-x)) & -Z_C \sinh(\gamma(l-x)) \\ -\sinh(\gamma(l-x))/Z_C & \cosh(\gamma(l-x)) \end{bmatrix} \begin{bmatrix} V_S \\ I_S \end{bmatrix} \tag{3}$$

where l is the length of the line. When a fault occurs d km away from the sending end, by making use of (2) and (3) the distance to the fault can be determined by:

$$d = \frac{1}{\gamma}\tanh^{-1}(A/B) \tag{4}$$

where

$$\begin{aligned} A &= V_S \cosh(\gamma l) - Z_C I_S \sinh(\gamma l) - V_R \\ B &= I_R Z_C + V_S \sinh(\gamma l) - Z_C I_S \cosh(\gamma l) \end{aligned} \tag{5}$$

For a three-phase system, the phase domain components are decomposed by making use of a modal transformation. In the present case, Clarke's transformation is used to convert the original phase variables into a set of *0*, α and β variables, as

M. Popov is with the Delft University of Technology, Faculty of EEMCS, Mekelweg 4, 2628 CD Delft, The Netherlands (e-mail: M.Popov@ieee.org),
G. Rietveld is with VSL Laboratory, Delft, The Netherlands (e-mail:G.Rietveld@vsl.nl).
Z. Radojevic is with Sungkyunkwan University, Suwon, Korea (e-mail: radojevic@ieee.org).
V. Terzija is with the University of Manchester, School of Electrical and Electronic Engineering, UK (e-mail: Vladimir.Terzija@manchester.ac.uk).

Paper submitted to the International Conference on Power Systems Transients (IPST2013) in Vancouver, Canada July 17-20, 2013

follows:

$$\begin{bmatrix} V_0 \\ V_\alpha \\ V_\beta \end{bmatrix} = T \begin{bmatrix} V_A \\ V_B \\ V_C \end{bmatrix}, \quad \begin{bmatrix} I_0 \\ I_\alpha \\ I_\beta \end{bmatrix} = T \begin{bmatrix} I_A \\ I_B \\ I_C \end{bmatrix}, \text{ where T=} \begin{bmatrix} 1 & 1 & 1 \\ 2 & -1 & -1 \\ 0 & \sqrt{3} & -\sqrt{3} \end{bmatrix} \quad (6)$$

where 0 stands for the ground mode, and α and β are the two areal modes. By applying the Clarke transformation, the single-phase solution can be extended to three-phase solution so that the characteristic impedance and the propagation constants can be expressed as:

$$Z_{C0} = \sqrt{(Z_s + 2Z_m)/(Y_s - 2Y_m)} = \sqrt{Z_0 / Y_0}$$
$$Z_{C\alpha} = Z_{C\beta} = \sqrt{(Z_s - Z_m)/(Y_s + Y_m)} = \sqrt{Z_1 / Y_1} \quad (7)$$

$$\gamma_0 = \sqrt{Z_0 Y_0}, \gamma_1 = \sqrt{Z_1 Y_1} \quad (8)$$

For the three modal components, the fault location can be expressed as:

$$d_i = \frac{1}{\gamma_i} \tanh^{-1}(A_i / B_i) \quad (9)$$

where A_i and B_i are:

$$A_i = V_{Si} \cosh(\gamma_i l) - Z_{Ci} I_{Si} \sinh(\gamma_i l) - V_{Ri}$$
$$B_i = I_{Ri} Z_{Ci} + V_{Si} \sinh(\gamma_i l) - Z_{Ci} I_{Si} \cosh(\gamma_i l) \quad (10)$$

and i=*0*, α or β which stand for the modal components of the signals.

III. Model Application

This section provides the results of the parameter dependent model application. For this, a combined section of line and cable is presented [7]. In the Netherlands, transmission network is constantly expanded by heavily loaded cables [8], which are placed in a mixed system consisting of lines and cables.

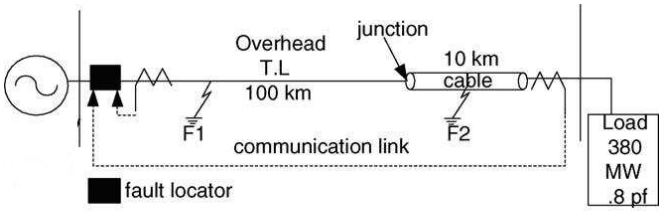

Fig. 1. Test network that consists of a 110 kV combined line-cable connection.

Table 1. Cable/line parameters

	R(Ω/km)	L(mH/km)	C(μF/km)
Transmission line (100 km)			
Z_1	0.3317	1.326	0.008688
Z_0	0.4817	4.595	0.004762
Cable (10 km)			
Z_1	0.412	0.4278	0.2811
Z_0	0.240	1.5338	0.1529

The efficiency of this model is seen in the fact that the fault locator does not show any problem because of the different line and cable parameters. For an arbitrary fault on the transmission line, the algorithm requires measured voltages and currents at the sending and receiving end. Because there is no busbar at the junction point between the line and the cable, the voltage/current at this point can be calculated by (2) or (3) depending on whether the fault is on the cable or line respectively.

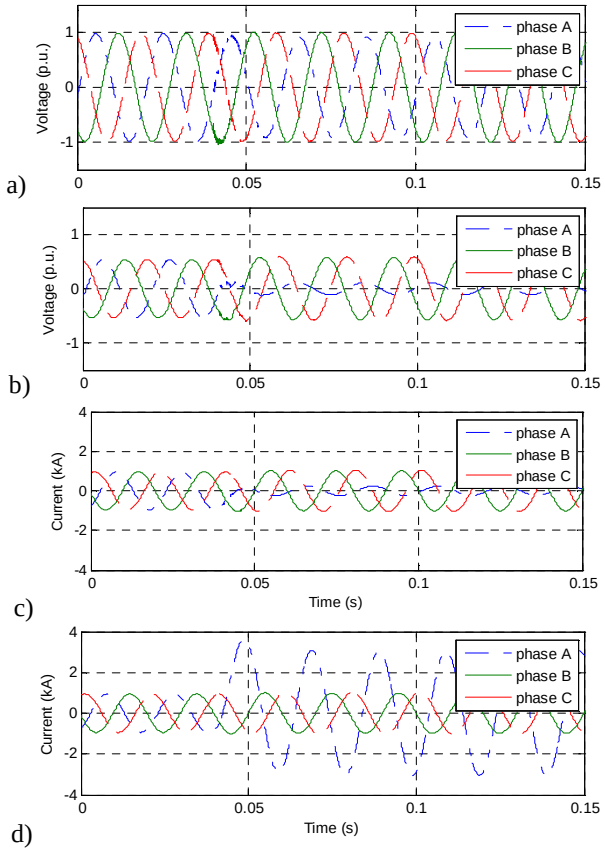

Fig.2 Voltage (p.u) and current (kA) waveforms during single-phase fault current at F1, 44.54 km from the sending end; a) phase voltages at the line sending end; b) phase voltages at the line receiving end; c) phase currents at the line receiving end; d) phase currents at the line sending end.

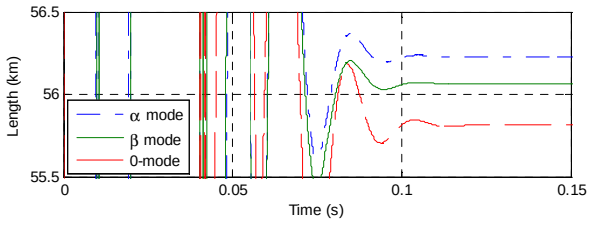

Figure 3. The result of the parameter dependent fault locator for a fault current on the line.

As it can be seen in Fig. 1, the voltages and currents are recorded at the remote ends of the line. For this case, two examples are taken into account.

The first is with a fault on the line and the second example is with a fault on the cable. Single-phase faults are taken in both cases, so that the application of the Clarke transformation is visible. A bolted fault current occurs 44 km from the line sending end at 0.04 ms. Since the transmission line is 100 km long, the fault occurs at 56 km from the receiving end

(junction point).

Fig. 2 shows line voltages and currents at the remote ends of the line. These waveforms are sampled with 256 samples per cycle and are used for the fault location. Discrete Fourier Transform has been used for the determination of the phasors. By making use of the Clarke transformation, three modes can also be used to locate the fault accordingly. In Fig. 3, the results of the α, β and 0 modes are illustrated. These modes provide 56.2 km, 56.06 km and 55.8 km for α, β and 0 mode respectively. This implies that the deviation of the fault location is 0.357 %, 0.107% and -0.357 %.

In Table 2, some results for different faults along the line are presented. The error is calculated with respect to the accurate fault location.

Table 2. Fault location along the line (single-phase fault)

Exact fault (km)	Calculated fault	Absolute Error (%)
15	15.006	0.040
30	30.011	0.016
50	49.983	0.034
70	70.021	0.030
85	85.019	0.022

The second example is a case for a fault that occurs on the cable. A single-phase fault current with 1 Ω fault resistance takes place at different locations along the cable.

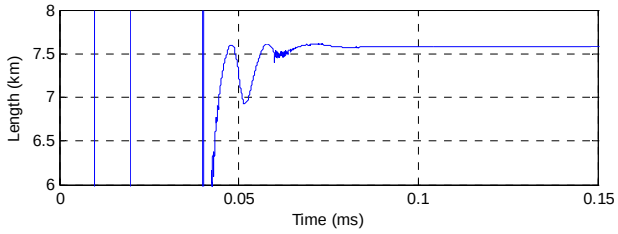

Fig. 4. An example of the fault location for a fault on the cable.

Fig, 4 illustrates the validity of the fault location algorithm. The calculated value is 7.58073 km against an accurate value of 7.58 km. The error in this case is 0.00963 %. Table 3 provides some results of the algorithm accuracy for faults along the cable.

Table 3. Fault location along the cable (single-phase)

Exact fault (km)	Calculated fault	Absolute Error (%)
2.42	2.4192	0.033
4.5	4.4985	0.033
7.3	7.2977	0.031
8.5	8.4973	0.031

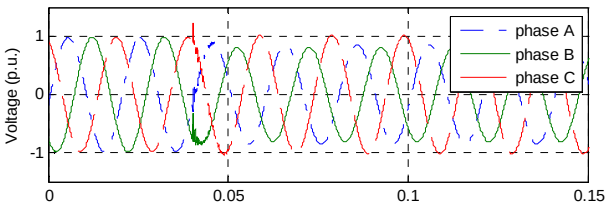

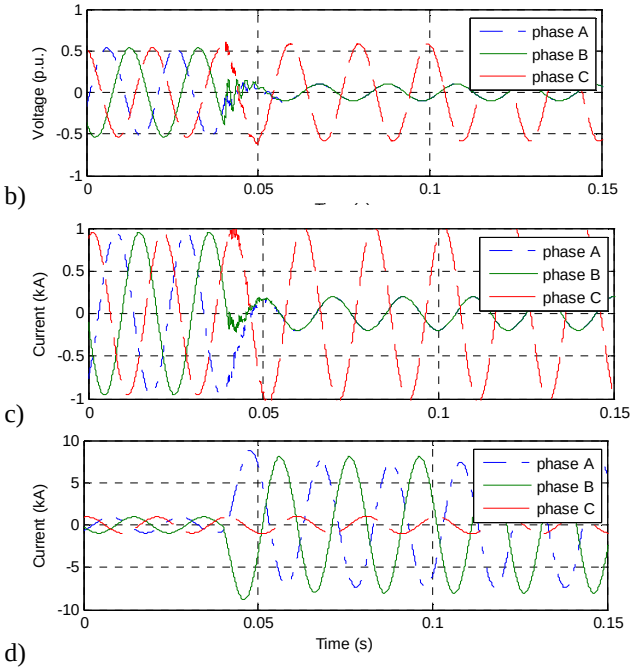

Fig.5 Voltage (p.u) and current (kA) waveforms during a double-phase fault current at 20 km from the line sending end; a) phase voltages at the line sending end; b) phase voltages at the line receiving end; c) phase currents at the line receiving end; d) phase currents at the line sending end.

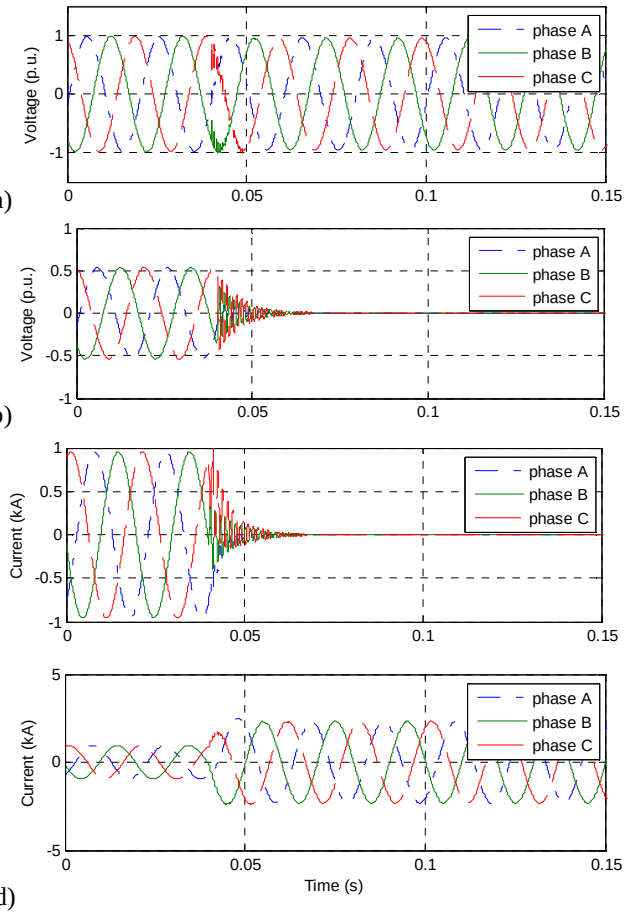

Fig.6 Voltage (p.u) and current (kA) waveforms during a three-phase

fault current at 85 km from the line sending end; a) phase voltages at the line sending end; b) phase voltages at the line receiving end; c) phase currents at the line receiving end; d) phase currents at the line sending end.

Fig. 5 and 6 show simulated voltages and fault currents during double and three phase fault currents respectively. The results of the fault location for a double phase and three phase fault current at different locations are presented in Table 4 and 5 respectively. In all cases the error is lower than 0.1%.

Table 4. Fault location along the line (double-phase fault)

Exact fault (km)	Calculated fault	Absolute Error (%)
20	20.004	0.004
30	30.004	0.013
50	49.993	0.014
70	70.011	0.015
85	85.012	0.014

Table 5. Fault location along the line (three-phase fault)

Exact fault (km)	Calculated fault	Absolute Error (%)
20	20.015	0.075
30	30.013	0.043
50	49.98	0.04
70	70.026	0.037
85	85.03	0.036

IV. Model Verification by Laboratory Measurements

In the previous sections, the two fault location algorithms were tested with simulated data, achieved by simulation of a power system fault using ATP-EMTP. This section describes further validation of the algorithms, using actual synchronized measurement data achieved in a setup by modeling a single phase power line.

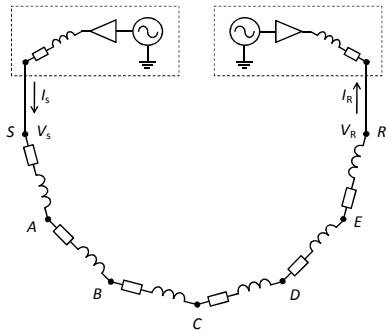

Fig. 7. Schematic setup for acquiring synchronized measurement data for the testing of fault location algorithms. The dashed boxes indicate the sending and receiving networks respectively. Faults have been successively applied at points A to E in the line S-R representing a HV overhead line.

The setup used for achieving fault location measurement data is schematically depicted in Fig. 7. The sending and receiving networks are realized by synchronized digital signal generators, power amplifiers, and air inductors. The two synchronized voltage sources each generate around 0.8 V_{rms}, which is amplified 25 times with two power amplifiers resulting in a voltage that is around 40 % of the output of VTs in actual HV networks. In order to simulate real networks with non-zero impedance, the output of the power amplifiers is connected to an air inductor, having both resistance and inductance. The dashed boxes in Fig. 7 indicate the two networks at the sending end (left) and receiving end (right) of the line respectively.

In this experiment, the single phase high-voltage line is simulated by a series connection of 6 air inductors. The inductors were chosen in a way that their inductance and internal resistance have relative values around Z = 0.2 + j 0.4 Ω/km, which is a typical value for HV lines. In this way 24 km of HV line was simulated. Zero ohm metallic shorts were made at the interconnections of the inductors simulating the HV line (points A – E) by connecting these points to ground during a measurement. The currents and voltages at the sending and receiving ends of the line (points S and R in Fig. 7) are synchronously measured using a four channel digitizer, with its internal 10 MHz clock locked to a cesium atomic clock. The actual currents and voltages are converted and scaled down to voltages suitable for the digitizer inputs using current probes and voltage dividers respectively. The signals are sampled at a rate of 25600 samples/sec (512 samples/period).

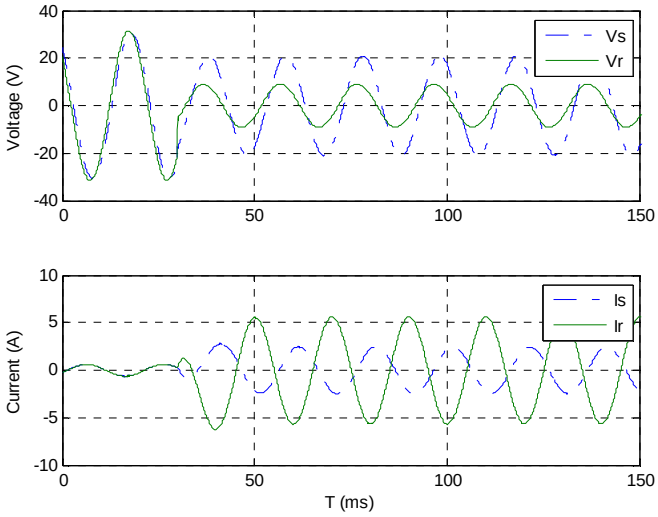

Fig. 8 Voltage (top) and current (bottom) as a function of time for a measurement using the model grid of fig. 7 when a fault occurs at point E in the HV line at t = 30.00 ms. Solid and dotted lines are for the sending and receiving end of the HV line respectively.

A typical example for the measurement results achieved with the setup is given in Fig. 8. In the stationary state at the start of the measurement, the voltage at the receiving end was 6.25 % higher, with 20° phase, with respect to the sending end. At t = 30.00 ms a fault occurs at point E in the line.

Table 6. Fault location in the measurements based on the impedance of the HV line, as well as deviations from this location with the locations determined by the two fault location algorithms

Fault location	Fault location (km)	Algorithm (km)	Error 2 (%)
A	4	3.95	1.25
B	8	7.98	0.25
C	12	12.07	0.58
D	16	16.15	0.93
E	20	20.15	0.75

Five measurements were performed with faults made at the 5 interconnections A – E between the inductors. The fault location in these five measurements, based on the total impedances of the line on the sending and receiving side of the line respectively, as well as those achieved through the algorithm.

Table 6 summarizes the results of the fault locations determined by the algorithm with that produced by the line impedance is somewhat worse than in the evaluation above and in earlier evaluations [2]. This has several reasons. First of all, the accuracy of the measurements is only around 0.5 – 1 %. This accuracy is mainly affected by the timing of the ADC cards, the accuracy of the voltage dividers and current probes, and the accuracy in the *L* and *R* measurement of the inductors simulating the line. Secondly, the fault location algorithm is based on transmission line equations that require capacitance in order to take into account the surge impedance and propagation constant. In this case, the value of the capacitance was taken to be the same as the line capacitance in the previous example. Fig. 9 shows an example of a simulated case according to Table 6.

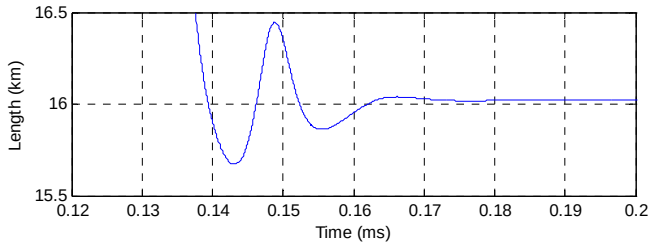

Fig. 9. Fault location according to parameter dependent algorithm for a fault case B of table 6. The fault is determined by evaluating the distance of the fault from the remote end.

V. Conclusion

The paper presents an accurate algorithm that can be used for fault location. The algorithm is based on the telegrafers' equations and requires the positive, negative and zero sequence impedance of the line and cable. In the present case, Clarke transformation is applied, however, one may use positive, negative and zero sequence symmetrical components in order to achieve the same results. The difference is the fact that the symmetrical component matrix consists of complex numbers whilst Clarke transformation matrix is real. Besides, Clarke transformation is traditionally known as very capable of dealing with transient studies, especially with fault location based on traveling waves [9]. The algorithm is checked for all types of faults that may occur in the combined line-cable system and can be efficiently used when the fault occurs either on the cable or the line. The algorithm presented only requires the measured voltages and currents at the sending and receiving end of the cable or line Since these parameters can be measured at the busbars (in Figure 1 this is denoted at the receiving end of the cable and the sending end of the line), the voltages and currents at the junction point can always be calculated using equations (2) or (3). Since it is not known in advance if the current is on the line or on the cable, the requested voltage and current of the junction point can be calculated using both the measured voltages and currents at the sending end of the line, and the measured voltages and currents at the receiving end of the cable. Consequently, two fault location algorithms executed in parallel determine the likely position of the fault in the line and in the cable. One of these positions is unrealistic, since the distance to the fault will be higher than the length of the line or cable. Since the algorithm presented in this paper only requires the terminal voltages and currents of the line or cable under study, it does not matter whether the remote end of the cable or line is a load or a source, at least not for low impedance faults.

In all cases the error is kept below 0.1%. The results are tested by making use of synchronised measurements in a laboratory environment. In the present case the authors were not able to provide actual line or cable so the measurements were done by making use of impedances that represent a line with a length of 24 km. However, the capacitances were ignored in the experimental case, which is one of the reasons that the error between the simulations and measurements is higher.

VI. Future Work

The future work will be based on the application of an algorithm [4] that does not make use of the line-cable parameters but only measurements. In this case, one may show if the capacitance of the line, cable or both plays a significant role in the error estimation. This type of modelling will be compared not only with the measurements but also with other existing models. The arc impedance in this case will also be taken into account. There are a lot of mixed cable-line connections that will be built in the near future in the Netherlands. This algorithm could be used for accurate fault detection in combined line-cable systems.

VII. References

1. A.A. Girgis, D.G. Hart, W.L. Peterson, A new fault location technique for two and three terminal lines, *IEEE Trans. Power Delivery* 7 (1) (1992) 98–107.
2. C.E. de Morais Pereira, L.C. Zanetta Jr, Fault location in transmission lines using one-terminal post-fault voltage data, *IEEE Trans. Power Deliv*ery. 19 (2) (2004) 570–575.
3. Z.Q. Bo, R.K. Aggarwal, A.T.Johns, A very accurate fault location and protection scheme for power cable using fault generated high frequency voltage transients, in *the Proceedings of the Eight Mediterranean Electro-technical Conference*, Industrial Applications in Power Systems, *MELECON 96*, Bari, Italy, May, 1996, pp. 777–780.
4. Z. M. Radojević, C. H. Kim, M. Popov, G. Preston, V. Terzija: New Approach for Fault Location on Transmission lines not Requiring Line Parameters, Presented at the *International Conference on Power Systems*

Transients (IPST2009) in Kyoto, Japan June 3-6, 2009.
5. M. Kezunovic, B. Kasztenny, Z. Galijasevic, Modeling, developing and testing protective relays using Matlab programmable relays and digital simulators, in: *Proceedings of the Third International Conference on Digital Power System Simulators*, ICDS '99, Vasteras, Sweden, May 1999.
6. M. Mohan Saha, R. Das, P. Verho, D. Novosel, Review of fault location techniques for distribution systems, in: Proceedings of the Power Systems and Communications Infrastructures for the Future, Beijing, September, 2002.
7. El Sayed Tag El Din, M. Mamdouh A. Aziz, D. Khalil Ibrahim, M. Gilany: Fault location scheme for combined overhead line with underground power cable, *Electric Power Systems Research* 76 (2006) 928–935.
8. TenneT: Ondergrondse kabels en bovengrondse hoogspanninglijnen: http://www.tennet.org/tennet/publicaties/position_papers/PP_Underground.aspx.
9. A. G. Phadke, J. S. Thorp: *Computer Relaying for Power Systems*, John Wiley & Sons Ltd, ISBN 978-0-470-05713-1, 2009.